Journal of Physiology (1989), **413**, *pp.* 139–157
With 10 *text-figures*
Printed in Great Britain

TRIPLE-BARREL STRUCTURE OF INWARDLY RECTIFYING K^+ CHANNELS REVEALED BY Cs^+ AND Rb^+ BLOCK IN GUINEA-PIG HEART CELLS

BY HIROKO MATSUDA, HIROSHI MATSUURA AND AKINORI NOMA

From the Department of Physiology, Faculty of Medicine, Kyushu University, Fukuoka 812, Japan

(*Received 11 July 1988*)

SUMMARY

1. The hypothesis that the inwardly rectifying K^+ channel consists of a triple-barrel structure was investigated. Inward currents were recorded under the blocking effects of external Cs^+ or Rb^+ in the cell-attached configuration of the patch-clamp technique using single ventricular cells enzymatically isolated from guinea-pig hearts.

2. Cs^+ (10–100 μM) or Rb^+ (20–100 μM) added to the 150 mM-K^+ pipette solution induced rapid open-blocked transitions in the inward open-channel currents. In about 20% of experiments the inward current showed two intermediate current levels equally spaced between the unit amplitude and the zero-conductance level. The current fluctuated between these four levels. In the remaining experiments no obvious sublevels were observed except spontaneous ones, whose amplitudes were not always equal to one-third or two-thirds of the unit amplitude.

3. In experiments showing sublevels, the probability that the open-channel current stayed at each level was measured at various concentrations of blockers and membrane potentials. In both Cs^+ and Rb^+ block, the distribution of the current levels showed reasonable agreement with the binomial theorem. This finding suggests that the inwardly rectifying K^+ channel is composed of three equally conductive subunits and each subunit is independently blocked by Cs^+ or Rb^+.

4. The dwell-time histogram in each substate was well fitted with a single-exponential function. On the assumption of the binomial model, the blocking (μ) and unblocking (λ) rate for Cs^+ and Rb^+ were calculated. The value of μ was linearly proportional to the concentration of the blocking ion at a given membrane potential and increased with hyperpolarization (e-fold increase with a change of $-43{\cdot}5$ mV in the Cs^+ block). λ was almost independent of the concentration of the blocking ion and less dependent on the membrane potential than μ.

5. The open and blocked times were calculated in experiments showing no clear sublevels. The mean open time was almost equal to the mean dwell time at the full open level in experiments showing sublevels under the same conditions. On the other hand, the mean blocked time was about two or three times longer than the mean dwell time at the zero-conductance level measured in experiments with sublevels.

These results may suggest that the instant one of the three subunits is plugged by blocking ions, the remaining two subunits are closed by unknown mechanisms.

6. Our results support the hypothesis that the cardiac inwardly rectifying K^+ channel is composed of three equally conductive subunits.

INTRODUCTION

The inwardly rectifying K^+ channel in guinea-pig ventricular cells loses its 'instantaneous' rectifying property when its inner mouth is exposed to low-Mg^{2+} solution (Matsuda, Saigusa & Irisawa, 1987; Vandenberg, 1987). Reapplication of Mg^{2+} causes the block of the outward current without affecting the inward current. Such a direction-dependent channel block by Mg^{2+} was also observed in the ATP-sensitive K^+ channel (Horie, Irisawa & Noma, 1987) and in the muscarinic receptor-operated K^+ channel (Horie & Irisawa, 1987). These effects are probably analogous to the voltage-dependent block of the inward current through the inwardly rectifying K^+ channel by external Cs^+, Rb^+ and Ba^{2+} (open-channel blockers; Hagiwara, Miyazaki & Rosenthal, 1976; Hagiwara, Miyazaki, Moody & Patlak, 1978; Standen & Stanfield, 1978, 1980; Ohmori, 1980; Fukushima, 1982).

Single-channel analysis of the inwardly rectifying K^+ current recorded in the presence of micromolar (2–10 μM) Mg^{2+} in the internal solution (Matsuda, 1988) has demonstrated that the outward current fluctuates between four equally spaced sublevels. Binomial analysis of probabilities for the subconductance states suggested that the channel is composed of three equally conductive units and each unit is independently blocked by Mg^{2+}. If so, the sublevels should appear in the inward current when the channel is blocked by open-channel blockers in the external solution. Previous workers, however, have not found sublevels in the presence of extracellular Cs^+ or Ba^{2+} (Kameyama, Kiyosue & Soejima, 1983; Sakmann & Trube, 1984*b*).

We re-evaluated the blocking effects of external Cs^+ and Rb^+ on the inward current through the inwardly rectifying K^+ channel, and found that the blockers induced two discrete subconductance levels in the inward currents in about 20% of experiments. Analysis of the sublevels supports the concept that the inwardly rectifying K^+ channel consists of a triple-barrelled structure. In the remaining experiments, the open-channel current rapidly fluctuated between the zero level and the unit amplitude. We propose that the block of one of the three units by Cs^+ or Rb^+ results in a concerted closure of the three conductive units that compose a single channel.

METHODS

Cell preparation

Single ventricular cells were isolated from guinea-pig (300–400 g) hearts using an enzymatic dissociation procedure (Powell, Terrar & Twist, 1980; Imoto, Ehara & Matsuura, 1987). Briefly, the guinea-pigs were deeply anaesthetized with sodium pentobarbitone (30 mg/kg, I.P.) and the chest was opened, under artificial respiration. The ascending aorta was cannulated *in situ* to start the coronary perfusion of the heart. The heart was excised and perfused via the aortic cannula with Tyrode solution, a Ca^{2+}-free Tyrode solution, and then 'digestive solution' at 37 °C. The digestive-solution contained 20 mg collagenase (Sigma, type I), 20 mg trypsin inhibitor (Sigma, type II-S), and 40 mg bovine serum albumin (Sigma, essentially fatty acid free) made up to 50 ml with Ca^{2+}-free

Tyrode solution, and was recirculated with a peristaltic pump for 25–30 min. The perfusates were filtered (Millipore, 0·45 μM). Thereafter collagenase was washed out with a high-K^+ storage solution (Isenberg & Klöckner, 1982). The left ventricle was then cut into small pieces in the storage solution and the dispersed ventricular cells were stored in the storage solution at room temperature.

Solutions

The composition of the Tyrode solution (mM) was: NaCl, 140; NaH_2PO_4, 0·33; KCl, 5·4; $CaCl_2$, 1·8; $MgCl_2$, 0·5; glucose, 5·5 and HEPES–NaOH buffer, 5 (pH = 7·4). The high-K^+ storage solution contained (mM): KCl, 120; succinic acid, 10; pyruvic acid, 5; $MgSO_4$, 5; taurine, 20; creatine phosphate, 5; K_2ATP (Sigma), 1; glucose, 20; EGTA, 0·2 and HEPES-KOH buffer, 10 (pH = 7·3). Pipette solution contained (mM): KCl, 140; $CaCl_2$, 2 and HEPES–KOH buffer, 5 (pH = 7·4). Stock solutions of 10 mM-CsCl and 10 mM-RbCl were prepared and an appropriate amount was added to the pipette solution to achieve final concentrations of 10–100 μM.

Recording technique

Patch electrodes were fabricated from glass capillaries (o.d., 1·5 mm; i.d., 1 mm) using a two-stage pull and were coated near their tips with silicone to reduce capacitance to ground. The tips were heat polished. These electrodes had tip resistances of 5–10 MΩ when filled with the pipette solution.

Ventricular cells were dispersed in a recording chamber mounted on the stage of an inverted microscope and superfused with Tyrode solution at 25 °C. The procedure of the single-channel recording was essentially the same as that described by Hamill, Marty, Neher, Sakmann & Sigworth (1981). Inward currents through the inwardly rectifying K^+ channel were recorded in the cell-attached configuration with a patch-clamp amplifier (EPC-7, List-electronic, Darmstadt, West Germany). Membrane potentials are expressed as voltage deviation from the resting membrane potential (E_r). In several experiments the pipette solution was exchanged using an intrapipette perfusion device (Soejima & Noma, 1984). To exchange solutions efficiently, electrodes with a lower resistance were used.

Data analysis

Data were stored on a magnetic video tape (Victor, video recorder BR6400, Tokyo) through a pulse-code modulator (NF, RP-882, Yokohama) and later played back through a four-pole low-pass Bessel filter (NF, FV-665, 48 dB/oct, Yokohama) with a −3 dB corner frequency of 0·8–1·0 kHz for computer analysis (NEC, PC-98XA, Tokyo). Currents were sampled every 0·1 ms (Cs^+ block) or every 0·2 ms (Rb^+ block), unless otherwise indicated. Gating and blocking kinetics were analysed in records where only one channel was active.

RESULTS

Flickering block of the inwardly rectifying K^+ channel by external Cs^+

In order to compare the channel gating kinetics in the presence of external Cs^+ with those of the control, inward single-channel currents were recorded continuously before and during the application of Cs^+ using the intrapipette perfusion device. Figure 1*A* gives the current changes caused by 10 μM-Cs^+ at E_r −40 or −60 mV. The amplitude of the current was not affected by Cs^+. The much denser trace clearly indicates that the duration of the open-channel current was cut short by the application of Cs^+. The long-lasting closures apparent in the control record disappeared 5 min after the application of Cs^+.

These effects of Cs^+ were analysed by constructing the open- and closed-time histograms illustrated in Fig. 1*B* and *C*. The distribution of open times was well fitted with a single-exponential curve in both cases, but the time constant was greatly reduced from 147 to 6·7 ms by the application of Cs^+. The latter value of the time constant corresponds to a blocking rate constant of 149 s^{-1}.

The distribution of closed times in the control showed at least two exponential components with time constants of 8·7 ms (Fig. 1*B*) and about 1 s. Usually the first or second bin (1 ms width) showed an excess number of events over the fitted curve. We neglected these short events and assumed that the channel has two closed states according to previous workers (Kameyama *et al.* 1983; Sakmann & Trube, 1984*b*). The major component of the closed-time histogram in the presence of Cs^+ was fitted with a single-exponential function having a time constant of 2·3 ms. Events longer than 25 ms were much fewer than in the control. Therefore, in the presence of Cs^+, the zero-current level mostly represents the blocked state rather than the closed state in the intrinsic channel gating.

In a simple model of channel gating in the presence of an open-channel blocker, transitions between states are described as:

$$C_2 \underset{\beta 2}{\overset{\alpha 2}{\rightleftharpoons}} C_1 \underset{\beta 1}{\overset{\alpha 1}{\rightleftharpoons}} O \rightleftharpoons B, \quad (1)$$

where C_1 and C_2 represent closed states, O the open state, and B the blocked state. If the blocking step ($O \rightharpoonup B$) is much faster than the transition $O \rightharpoonup C_1$, the channel should show a longer mean burst time in the presence of blocker than the mean open time in the absence of the blocker (Neher, 1983). This was tested by constructing a histogram for burst time in the presence of Cs^+. A burst time was defined as a period of successive opening and closing, during which no closed time was longer than three times the time constant of the closed-time histogram (2·3 ms). The time constant of 334 ms of the exponential distribution was about 2·5 times longer than the mean open time (147 ms) in the control. Essentially the same results of the open- and closed-time distributions were obtained in three other experiments, thus supporting the concept of the open-channel block by Cs^+.

In two experiments, sublevels of the open-channel current were induced by 20 μM-Cs^+ applied using the intrapipette perfusion device (Fig. 2). This patch contained at least five channels, and unitary currents overlapped in the control record (upper panel). In one channel, the application of Cs^+ induced sublevels spaced by one-third of the unit amplitude. The other channels showed simple open–blocked transitions, and were closed in the record shown in the lower panel.

To simplify the experimental procedure, Cs^+ or Rb^+ was added to the pipette solution before seal formation without using the perfusion device in the following experiments.

Subconductance states revealed by Cs^+ and Rb^+

Sublevels of the inward open-channel currents were induced in seven (16%) out of forty-four experiments with 10–100 μM-Cs^+, and in four (20%) out of twenty

Fig. 1. Current changes induced by Cs^+ applied in the patch electrode. *A*, single-channel currents (lower trace) were recorded from the same patch before and during perfusion of the patch electrode with the solution containing 10 μM-Cs^+. The upper trace indicates the membrane potential. The time after the start of perfusion with Cs^+ is indicated at the top. *B*, inset shows a current record obtained at E_r −60 mV before the application of Cs^+. The histograms of the open times (left) and the closed times (right) were fitted with a single-exponential function with the time constants indicated. Time bins of histograms are 20

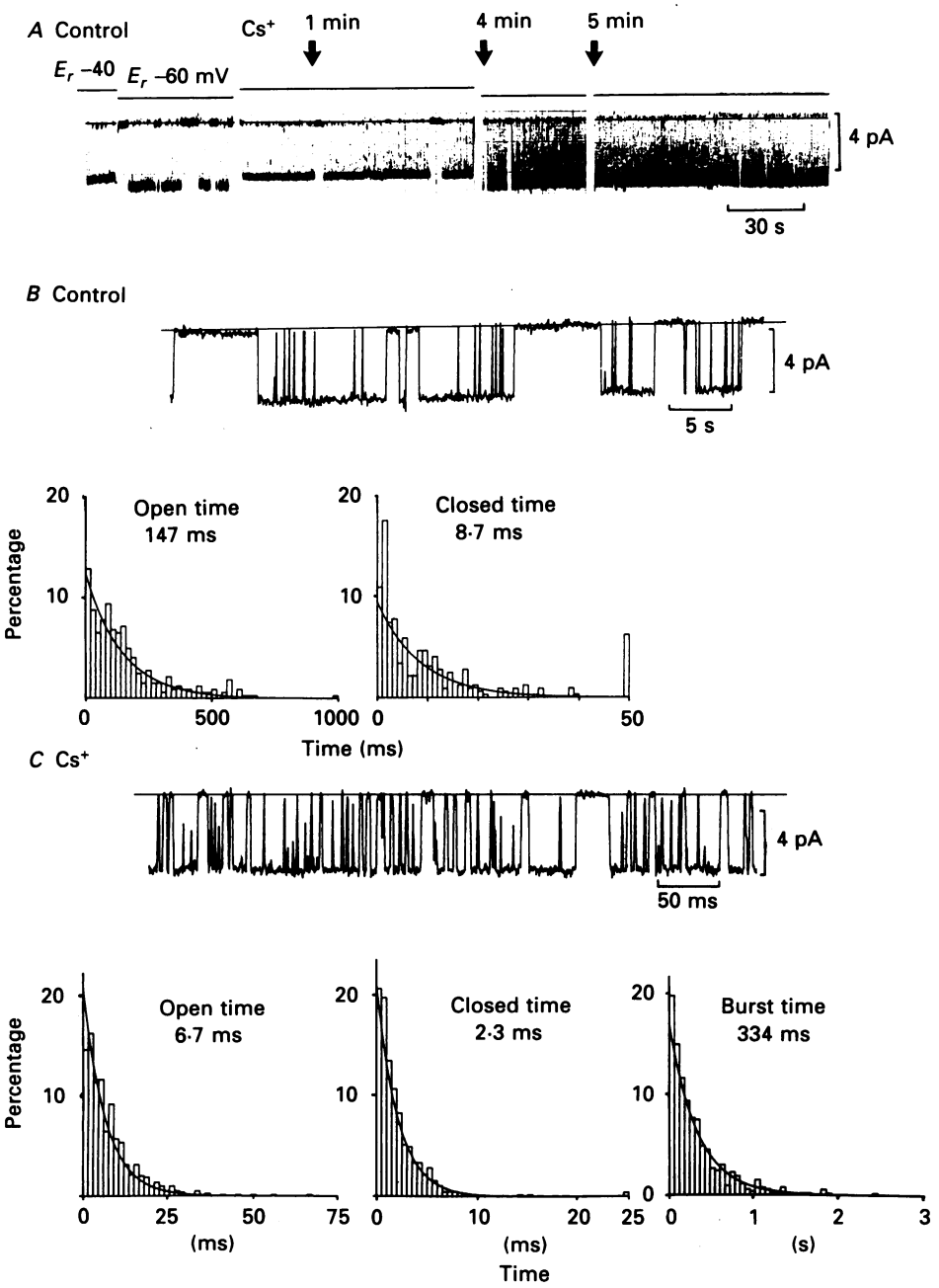

ms for the open times and 1 ms for the closed times. Currents were sampled every 0·5 ms. The number of events is 319 in both histograms. *C*, current record was obtained at E_r −60 mV 5 min after the start of 10 μM-Cs^+ perfusion and illustrated at a faster time scale than in *B*. Currents were sampled every 0·5 ms. Histograms of the open times (left), closed times (middle) and burst times (right) were fitted with a single-exponential function with the time constants indicated. The bin width is 1·5 ms for open time, 0·5 ms for the closed time, and 60 ms for burst time. The number of events was 788 in the open time, 1022 in closed time and 538 in burst time.

experiments during the application of 20–100 μM-Rb^+. In other experiments, as shown in Fig. 1*C*, simple transitions between the zero-conductance level and the full open level were observed, independent of the concentrations of blockers. Since some patches contained more than one channel, channels showing sublevels are likely to represent less than 20% of the whole population of inwardly rectifying K^+ channels.

Figure 3 shows representative records of sublevels induced in the inward currents by Cs^+ (Fig. 3*A*) and Rb^+ (Fig. 3*C*) at different membrane potentials. The sublevels

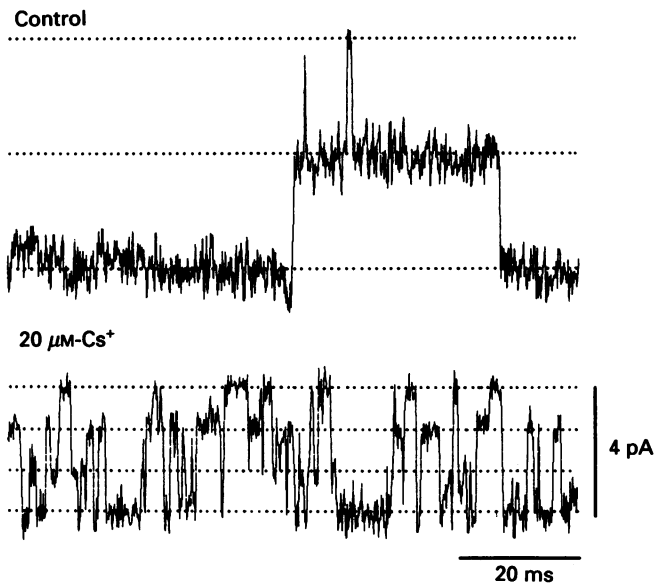

Fig. 2. Sublevels of the open-channel current induced by 20 μM-Cs^+ applied using the pipette perfusion device. The upper record was obtained before the application of Cs^+. This patch contained at least five channels. The dotted lines indicate, from the top, levels at which three, four and five channels are open. Because of multi-channel recording the noise of the current is relatively large. The lower record was obtained about 20 min after the application of 20 μM-Cs^+ when other channels, showing no sublevels, were temporarily closed. Dotted lines indicate levels of 0, one-third, two-thirds and full open-channel current. Holding potential E_r −40 mV; filter 1·5 kHz.

were equally spaced at intervals of one-third of the maximum open-channel current as indicated by the dotted lines. It is evident that the inward currents through a single inwardly rectifying K^+ channel fluctuate between four well defined sublevels at all membrane potentials. The current–voltage (*I–V*) relations for each level were shown in the lower panels (Fig. 3*B* and *D*). The slope conductance of the maximum open-channel current was 30 pS (Fig. 3*B*) and 33 pS (Fig. 3*D*). These values are in agreement with the previous reports of the single-channel conductance at 140 mM external K^+ (Sakmann & Trube, 1984*a*; Kurachi, 1985) and rule out the possibility that unitary currents of three separate channels overlapped resulting in apparent 'sublevels'. The lines drawn using one-third and two-thirds of the unit slope conductance fit the data points of the sublevels. We conclude that there are three

equally conductive units within a channel, each of which can be independently blocked by Cs^+ or Rb^+.

In experiments where the current flickered mostly between the zero-conductance level and full open level, sublevels with one-third and two-thirds of the unit conductance appeared only occasionally.

Binomial distribution of the sublevels

If the inwardly rectifying K^+ channel is composed of three equally conductive units and each unit is blocked (plugged) by the blocking ions independent of the

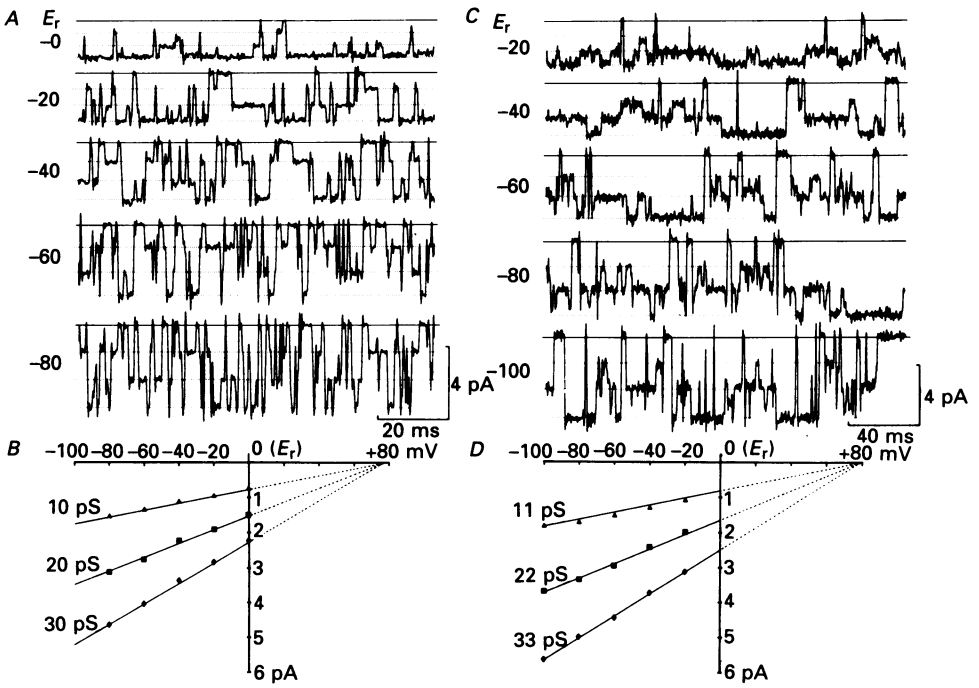

Fig. 3. *A* and *C*, subconductance states revealed by 20 μM external Cs^+ (*A*) and 100 μM-Rb^+ (*C*). Numerals to the left of each trace refer to the holding potential. Continuous lines show the zero-current level and the dashed lines are drawn at levels of one-third, two-thirds and full open-channel current. Currents were low-pass filtered at 2 kHz. *B* and *D*, *I–V* relation of open-channel substates obtained from the patches shown in *A* (*B*) and *C* (*D*). The lines drawn using one-third and two-thirds of the unit slope conductance fit the data points of sublevels well.

others, the probability that the single-channel current remains at zero (P_0), one-third (P_1), two-thirds (P_2) and full open (P_3) of the unit amplitude should be described by a binomial distribution. The mean open-channel current was measured from records during the burst as shown in Fig. 3, and the probability of one subunit being open (p) was calculated by dividing the mean open-channel current by the unit amplitude.

Amplitude histograms were constructed to estimate the probability of the current remaining at each level. Figure 4*A* shows amplitude histograms in the presence of 20 μM-Cs^+ and Fig. 4*C* those in the presence of 100 μM-Rb^+. Four peaks were clearly recognized at each membrane potential. When the membrane potential was made

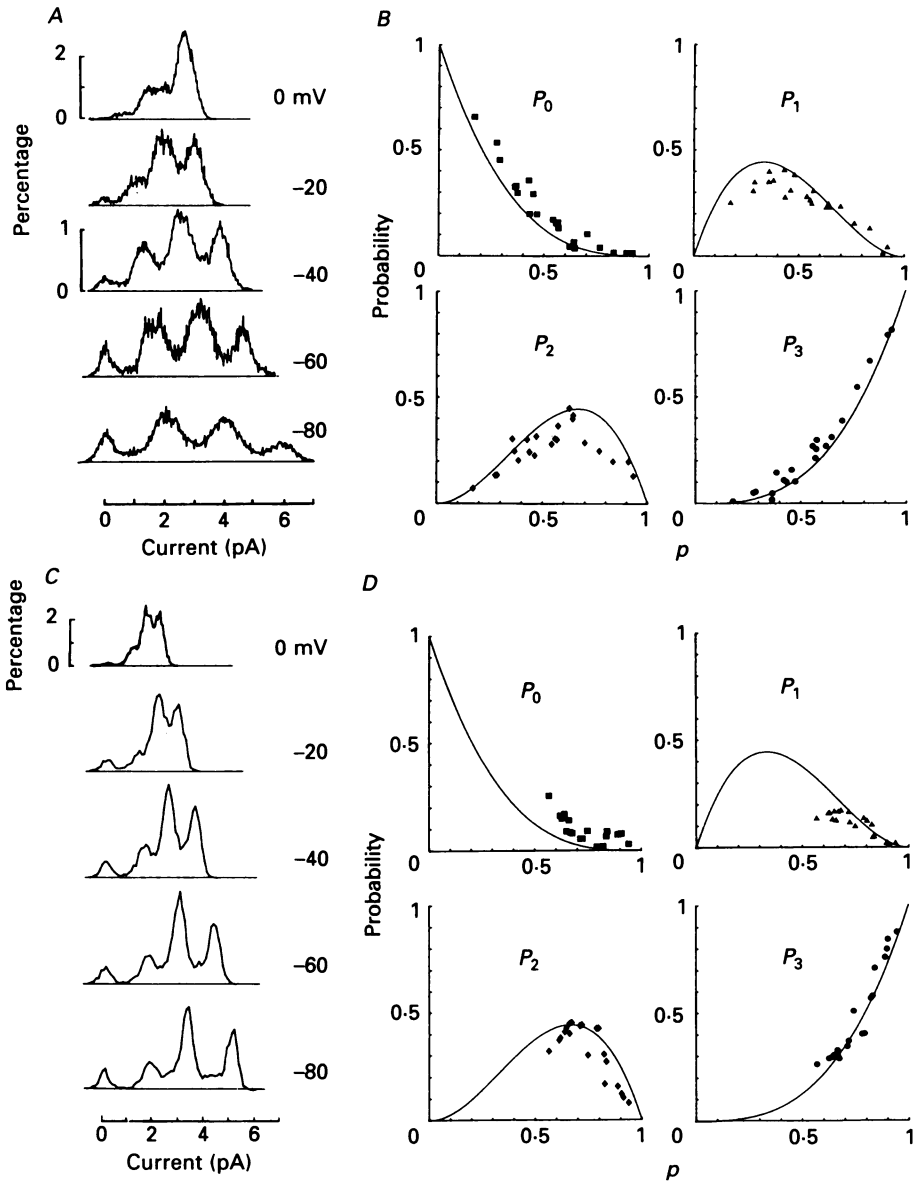

Fig. 4. Binomial analysis of the substate probabilities. *A* and *C*, amplitude histograms constructed from a record of 1·6 s in duration with 20 μM-external Cs^+ (*A*) and from a record of 3·2 s with 100 μM-Rb^+ (*C*). The ordinate gives density of distribution in percentage with a bin width of 0·05 pA. Membrane potentials are indicated to the right of each histogram as the deviation from the resting potential. The probability of one subunit being open (p) was, from top to bottom: 0·85, 0·75, 0·64, 0·57 and 0·48 in *A*, and 0·80, 0·73, 0·72, 0·68 and 0·65 in *B*, respectively. *B* and *D*, distribution of sublevels obtained in six experiments for Cs^+ block (*B*) and in four experiments for Rb^+ block (*D*). The Cs^+ concentrations used were 10, 20, 40 and 100 μM and the Rb^+ concentrations were 20, 50 and 100 μM. The probability of each substate was calculated from the relative height of each peak, instead of the area underlying the curve, and were plotted against p together with the theoretical curve. The theoretical curves in each panel were drawn from the following equations: $P_0 = (1-p)^3$, $P_1 = 3p(1-p)^2$, $P_2 = 3p^2(1-p)$ and $P_3 = p^3$.

more negative, the probability of observing zero or one-third level increased progressively at the expense of the probability of observing two-thirds and full size level (see also Fig. 3*A* and *C*). In this experiment p was reduced from 0·85 to 0·43 in Cs^+ block and from 0·80 to 0·62 in Rb^+ block by hyperpolarizing the membrane by 100 mV from E_r.

P_0, P_1, P_2 and P_3 were estimated from the relative height of each peak and plotted against p in Fig. 4*B* (Cs^+ block) and Fig. 4*D* (Rb^+ block). In both cases, the data points seem to be distributed along the theoretical curves. In the case of Rb^+ block (Fig. 4*D*), the values of P_0 were mostly higher than those predicted by the binomial theorem. This might be because the zero-current level used for the calculation might include not only the blocked state, but also the closed state of the channel. Because the blocking kinetics of Rb^+ were not much faster than the intrinsic gating kinetics, they were difficult to separate.

Kinetics of Cs^+ and Rb^+ block with sublevels

The above binomial analysis of the probability of remaining at each current level indicates that each subunit is blocked independently of the other subunits composing the same channel. If the block of each subunit is described as:

$$\text{open} \underset{\lambda}{\overset{\mu}{\rightleftharpoons}} \text{blocked}, \tag{2}$$

where λ is the first order unblocking rate and μ is the blocking rate given by the product of the second-order rate constant and the concentration of blocker, p is expressed as $\lambda/(\mu+\lambda)$ and transitions between substates during the open state of the channel is described as:

$$O_3 \underset{\lambda}{\overset{3\mu}{\rightleftharpoons}} O_2 \underset{2\lambda}{\overset{2\mu}{\rightleftharpoons}} O_1 \underset{\lambda}{\overset{\mu}{\rightleftharpoons}} O_0, \tag{3}$$

where O_3, O_2 and O_0 represent the substates in which three, two, one and none of the subunits are free from the blocking ions, respectively. In this model, the mean lifetimes in the substates are given as:

$$\tau_0 = \tfrac{1}{3}\lambda, \tag{4}$$

$$\tau_1 = 1/(2\lambda+\mu), \tag{5}$$

$$\tau_2 = 1/(\lambda+2\mu), \tag{6}$$

and

$$\tau_3 = \tfrac{1}{3}\mu, \tag{7}$$

where τ_0, τ_1, τ_2 and τ_3 represent the mean lifetimes in O_0, O_1, O_2 and O_3, respectively.

Lifetimes or dwell times in each substate were measured by setting a threshold level at around half of the open level of the subunits. Figure 5*A* shows the dwell-time histograms in each substate with 20 μM-Cs^+ at E_r −40 mV, and Fig. 5*B* those with 100 μM-Rb^+ at E_r −80 mV. In both cases the histogram could be fitted with a single-exponential function. In Rb^+ block an excess number of events longer than 10 ms were observed in O_0 above the fitted curve. This may indicate that the zero-

conductance level associated with the closed states of the channel (C_1 and C_2 in eqn (1)) was included in the analysis as suggested earlier.

Table 1 summarizes measurements of the time constants at different membrane potentials in the experiment shown in Fig. 5*A*. Values of μ and λ were determined from τ_0 and τ_3, respectively. Theoretical values of τ_1, τ_2 and p were calculated using μ and λ and are shown in parentheses. These values are in good agreement with the experimental values.

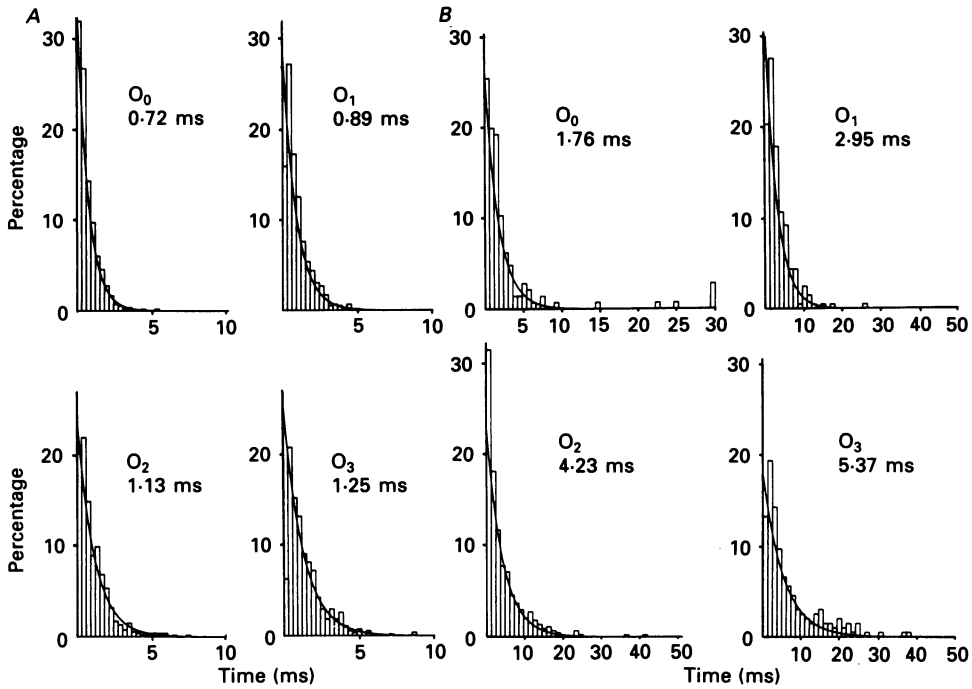

Fig. 5. Dwell-time histograms in each substate in Cs^+ block (*A*) and Rb^+ block (*B*). *A*, the histogram was formed in 0·3 ms bins and fitted with a single-exponential function with time constants indicated. The number of events were 544 in O_0, 593 in O_1, 525 in O_2, and 540 in O_3. Cs^+, 20 μM; voltage, E_r −40 mV. *B*, the histogram was formed in 0·6 ms bins in O_0 or 1·2 ms bins in O_1, O_2 and O_3 and fitted with a single-exponential function with time constants indicated. The number of events were 146 in O_0, 207 in O_1, 435 in O_2 and 197 in O_3. Rb^+, 100 μM; voltage, E_r −80 mV.

μ and λ for Rb^+ block were estimated from τ_2 and τ_3 (Table 2), because estimation of τ_0 might be erroneous due to difficulty in discrimination O_0 from the closed state of the channel. μ and λ determined in this way again accurately predicted τ_0, τ_1 and p.

Blocking and unblocking rates obtained at different potentials and concentrations of the blocking ions were plotted on a semi-logarithmic scale against the membrane potential (Fig. 6). The blocking rate μ increased linearly with increasing Cs^+ or Rb^+ and exponentially with more negative potentials. In general, the rate constant k is given as,

$$k = k_0 \exp(z \delta E F/R T), \tag{8}$$

TABLE 1. Kinetic analysis of substates with 20 μM-Cs^+

Potential (mV)	τ_0 (ms)	τ_1 (ms)	τ_2 (ms)	τ_3 (ms)	p	μ (s^{-1})	λ (s^{-1})
E_r −0	0·76	0·80	1·67	4·09	0·85	81·5	439
		(1·04)	(1·66)		(0·84)		
E_r −20	0·79	0·99	1·35	2·34	0·77	142	422
		(1·01)	(1·42)		(0·75)		
E_r −40	0·72	0·89	1·13	1·25	0·64	267	463
		(0·84)	(1·01)		(0·63)		
E_r −60	0·73	0·80	0·82	0·93	0·57	358	457
		(0·79)	(0·85)		(0·56)		
E_r −80	0·75	0·74	0·74	0·72	0·48	463	444
		(0·73)	(0·73)		(0·49)		
E_r −100	0·76	0·69	0·60	0·54	0·43	617	439
		(0·67)	(0·60)		(0·42)		

μ and λ were calculated from τ_0 and τ_3. τ_1, τ_2 and p, calculated using these values, are listed in parentheses.

TABLE 2. Kinetic analysis of substates with 100 μM-Rb^+

Potential (mV)	τ_0 (ms)	τ_1 (ms)	τ_2 (ms)	τ_3 (ms)	p	μ (s^{-1})	λ (s^{-1})
E_r −0	2·31	2·69	4·38	8·06	0·81	41·3	146
	(2·28)	(3·00)			(0·78)		
E_r −20	2·33	3·15	4·71	7·36	0·73	45·3	122
	(2·73)	(3·46)			(0·73)		
E_r −40	2·81	3·18	4·79	6·94	0·72	48·0	113
	(2·95)	(3·65)			(0·70)		
E_r −60	2·72	3·55	4·44	5·53	0·68	60·3	105
	(3·17)	(3·70)			(0·64)		
E_r −80	1·76	2·95	4·23	5·37	0·65	62·1	113
	(2·94)	(3·47)			(0·65)		
E_r −100	2·41	2·42	3·77	4·46	0·63	74·7	116
	(2·87)	(3·26)			(0·61)		

μ and λ were determined from τ_2 and τ_3. The theoretical values of τ_0, τ_1 and p are listed in parentheses.

where k_0 is the rate constant at 0 mV, z the valency of the blocking ion, E the membrane potential and δ a factor representing the efficiency of membrane potential. R, T and F are the thermodynamic constants with their usual meanings. δ was 0·59 in Cs^+ block (Fig. 6*A*), and 0·14 in Rb^+ block (Fig. 6*B*), indicating that the voltage dependence of block is more marked in Cs^+ block than in Rb^+ block. The blocking rate of Cs^+ was larger than that of Rb^+ by a factor of about 10.

The unblocking rate λ was almost independent of the concentration of Cs^+ or Rb^+. The membrane potential affected Cs^+ block in a complicated manner: it decreased with hyperpolarization from E_r −0 to −60 mV ($\delta = -0{\cdot}34$), but slightly increased with further hyperpolarization from E_r −60 to −100 mV (Fig. 6*A*). The unblocking rate of Rb^+ was smaller by a factor of 4 compared with that of Cs^+ and showed no obvious voltage dependence (Fig. 6*B*).

Blocking kinetics in the absence of sublevels of the open-channel currents

In most of the experiments, the application of Cs^+ or Rb^+ induced no sublevels; the open-channel current fluctuated between the zero-conductance level and the full open level. We measured the mean open and blocked times at different membrane potentials and Cs^+ concentrations (Figs 1*B* and 8*A*) and calculated the blocking and unblocking rates, which were given as the reciprocal of the time constants. As in patches with sublevels, the blocking rate was almost linearly proportional to the

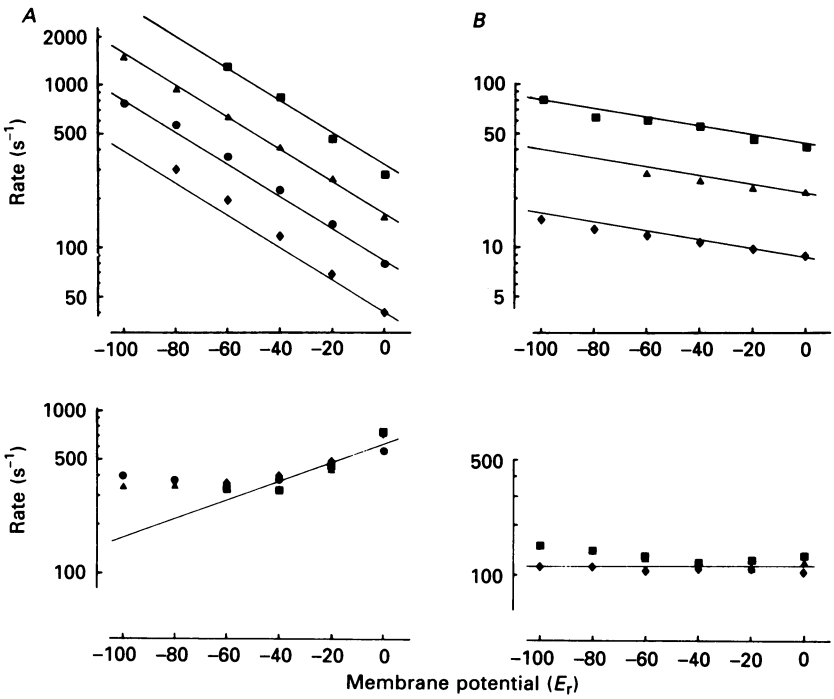

Fig. 6. Blocking and unblocking rates for Cs^+ (*A*) or Rb^+ block (*B*) measured in experiments showing sublevels. Data points represent the mean value of two experiments. Deviations from the mean value were less than 10% of the mean. Blocking (upper panel) and unblocking (lower panel) rates were plotted in a semilogarithmic scale against membrane potential for 10 (◆), 20 (●), 40 (▲) and 100 μM (■) Cs^+ and 20 (◆), 50 (▲) and 100 μM (■) Rb^+. The voltage-dependent change of the blocking rates was fitted with a straight line having a slope of $\delta = 0{\cdot}59$ (Cs^+) and $\delta = 0{\cdot}14$ (Rb^+). The line for the unblocking rate by Cs^+ has a slope of $\delta = -0{\cdot}34$.

concentration of Cs^+ and increased exponentially with hyperpolarization of the membrane, giving the value of $\delta = 0{\cdot}59$ (upper panel of Fig. 7). Note that the blocking rate is approximately three times larger than μ in the experiments with sublevels at the comparable condition (Fig. 6*A*; see next section).

The unblocking rate was independent of the Cs^+ concentration and showed a voltage dependence similar to that in experiments showing sublevels. The unblocking rate decreased first with hyperpolarization ($\delta = -0{\cdot}34$) and then increased with further hyperpolarization (Fig. 7). It should be noted that the values of δ for the

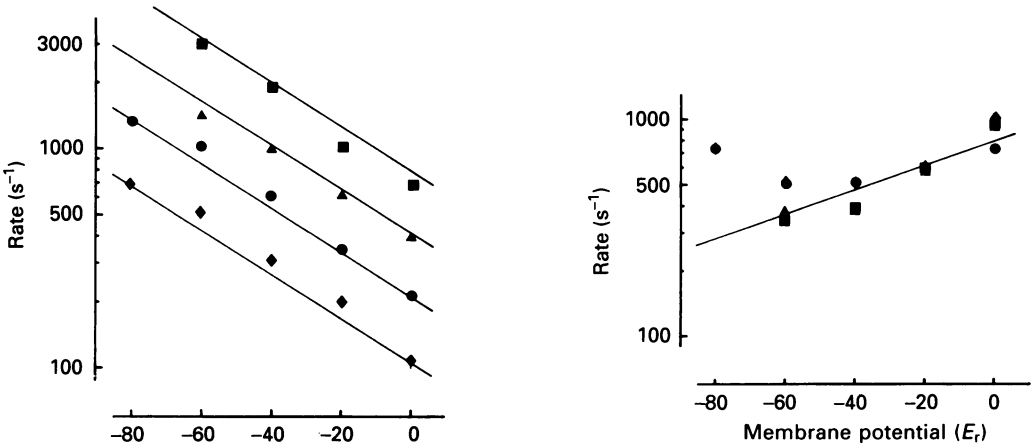

Fig. 7. Blocking (left graph) and unblocking (right graph) rates in experiments without sublevels. 10 (◆), 20 (●), 40 (▲) and 100 μM (■) of Cs^+. Every symbol represents mean values of two experiments. The slope of the straight line was $\delta = 0{\cdot}59$ in left and $\delta = -0{\cdot}34$ in right panel.

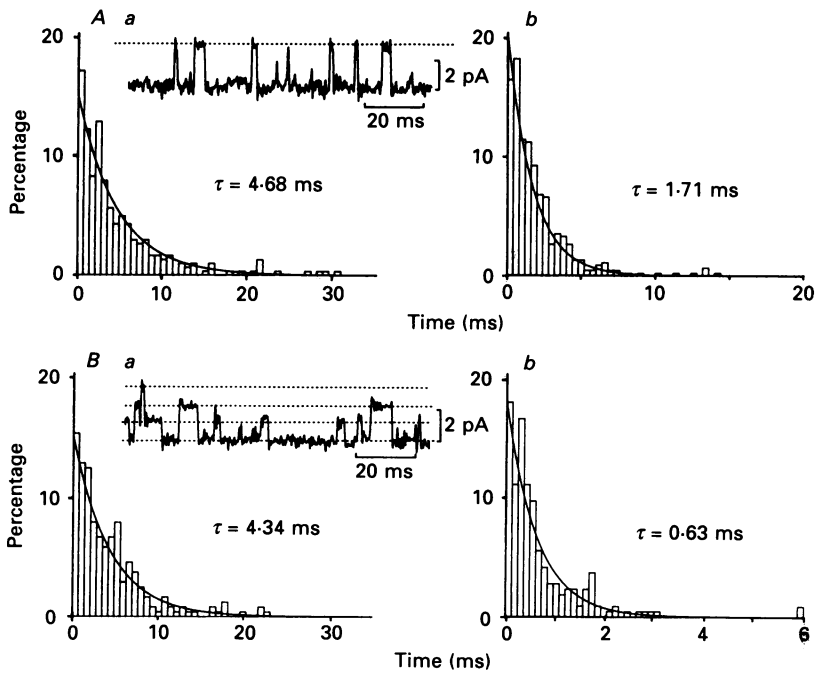

Fig. 8. *A*, histograms of the open time (*a*) and blocked time (*b*) in an experiment showing no sublevels. *B*, histogram of the dwell time at the full open level (*a*) and zero-conductance level (*b*) in an experiment showing distinct sublevels. Both sets of data were obtained at E_r −20 mV with 20 μM-Cs^+. The time constants of the exponential distribution and a part of the current record are indicated. Time bins of histograms are 0·7 ms for the open time, 0·4 ms for the blocked time in *A* and 0·12 ms for the zero-conductance time in *B*. The number of events ranged from 217 to 456.

blocking and unblocking rates are in good agreement with those obtained in experiments with distinct sublevels. Essentially the same result was obtained in the Rb^+ block where no distinct sublevels were observed.

Relevance of the triple-barrel model for the block that does not show sublevels

Sublevels induced by external Cs^+ or Rb^+ in the inward current were observed only in less than 20% of the channels. However, since sublevels were seen in the outward current in all channels to which internal Mg^{2+} was applied (Matsuda, 1988), we tried to interpret the present result on the basis of the triple-barrel model. In Fig. 8, the open- and blocked-time histograms obtained in a patch showing no sublevels were compared with the dwell-time histograms in O_3 and O_0, respectively, obtained

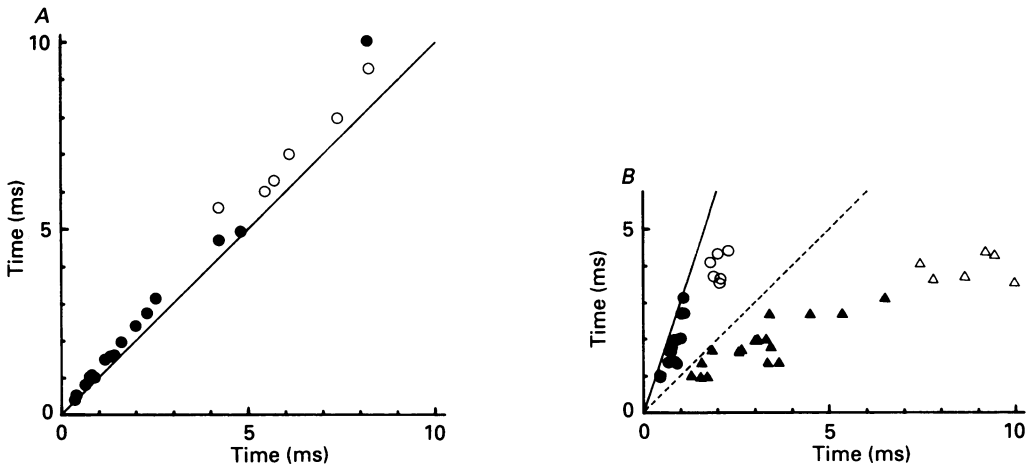

Fig. 9. *A*, mean dwell times at the full open level in experiments with sublevels (abscissa) were compared with the mean open times in experiments without sublevels (ordinate). Each point was obtained at the same potential and concentration of the Cs^+ (●) or Rb^+ (○). The slope of the line is 1. *B*, mean times at the zero-conductance level in experiments with sublevels (abscissa) and those in experiments without sublevels (ordinate). The continuous line has a slope of 3. Another model (eqn (10)) tested in the Discussion is also shown: (▲), Cs^+ block; (△) Rb^+ block.

from another patch showing sublevels at the same membrane potential and Cs^+ concentration. τ_3 is very similar to the mean open time without sublevels. τ_0 is about one-third of the mean blocked time in the absence of sublevels.

The results are summarized in Fig. 9. In each panel, the ordinate is the dwell time in experiments without sublevels and the abscissa gives that in experiments showing sublevels. Each point in Fig. 9 represents the mean experimental value obtained at the same concentration of Cs^+ or Rb^+ and at the same membrane potential. The data points for the open time lie on a straight line with a slope of 1, indicating that the dwell times coincide between these two groups.

The coincidence of the amplitude of the full open-channel current, voltage dependence of the blocking and unblocking rates (δ) and the dwell times at the full open level led us to assume that, in cases without sublevels, some gating mechanism simultaneously shuts the triple-barrel channel if one of the three subunits is blocked.

In this situation the transition between the channel states can be described as follows, instead of as in eqn (3):

$$O \underset{\lambda}{\overset{3\mu}{\rightleftharpoons}} B \tag{9}$$

where O and B represent the open (unblocked) and blocked state, respectively. This model predicts that the mean open time is identical to τ_3 and that the mean lifetime of the blocked state is three times as long as τ_0. This was tested in Fig. 9*B*, where all data points for the blocked states (circles) were distributed near the straight line with a slope of 3, but were clearly below the line.

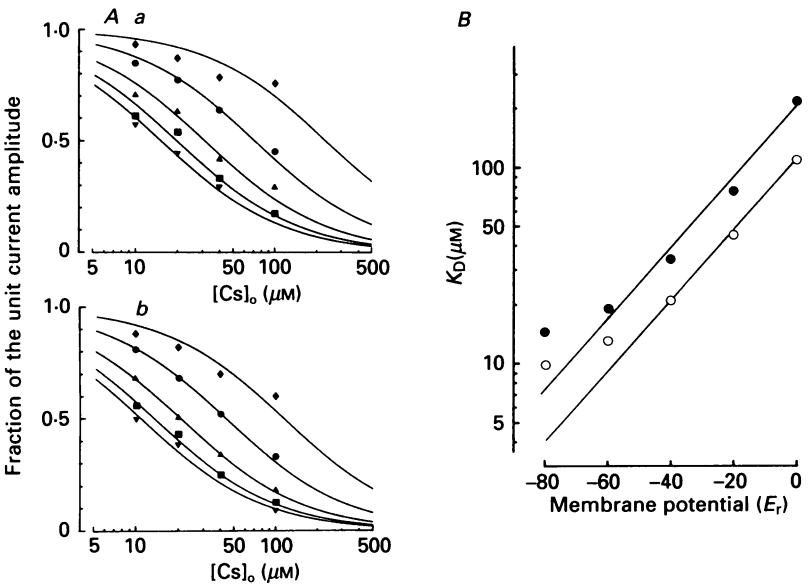

Fig. 10. *A*, the mean patch currents expressed as a fraction of the unit current amplitude are plotted against the concentration of Cs^+ in the experiment with sublevels (*a*) and in that without sublevels (*b*). ◆, for E_r; ●, for E_r −20 mV; ▲, for E_r −40; ■, for E_r −60; ▼, for E_r −80 mV. The continuous lines are drawn assuming a Hill coefficient of 1, with dissociation constants, from top to bottom, of 210, 80, 35, 20 and 15 μM in (*a*) and those of 105, 45, 20, 12 and 10 μM in (*b*). *B*, dependence of the apparent dissociation constant (K_D for Cs^+ on membrane potential in the experiment with sublevels (●) and in that without sublevels (○).

The two different models, eqns (3) and (9), give different dissociation constants (K_D), which are λ/μ and $\lambda/3\mu$, respectively. The mean patch current expressed as a fraction of the unit amplitude is plotted against the concentration of Cs^+ for each membrane potential, with (Fig. 10*Aa*) and without sublevels (Fig. 10*Ab*). Saturation kinetics with a Hill coefficient of 1 gave a reasonable fit in both cases and the values of the apparent dissociation constant were determined from the fitted curve. The relationship between the apparent dissociation constant and the membrane potential is shown in Fig. 10*B*. The dissociation constant in the experiment with sublevels is twice that without sublevels. Thus, eqn (9) cannot explain the results completely. An alternative mechanism will be discussed in the Discussion.

DISCUSSION

The present study demonstrated that external Cs^+ or Rb^+ induced sublevels of one-third and two-thirds of the unit amplitude in the inward single-channel currents. The probability of remaining at these sublevels can be well described by the binomial theorem as in the block of outward currents by internal Mg^{2+} (Matsuda, 1988). In our preliminary experiments, application of external Ba^{2+} also revealed sublevels of one-third and two-thirds of the unit amplitude (H. Matsuda, H. Matsuura and A. Noma, unpublished observation). It is well established that Cs^+, Rb^+ and Ba^{2+} are open-channel blockers of the inwardly rectifying K^+ channel (for references see the Introduction). In fact, the blocking rate in the experiments showing sublevels was exponentially voltage dependent (Fig. 6), and the block by internal Mg^{2+} is unidirectional (Matsuda *et al.* 1987; Vandenberg, 1987; Matsuda, 1988). These observations favour the view that the blocking ions plug the triple ionic pathways of the channel to induce sublevels.

Another possible mechanism that may induce sublevels is the binding of the blocking ions to a receptor site on the channel protein leading to different conductive states of a single-barrel channel. However, this is much less likely since it seems unrealistic to assume such binding sites both on the inside of the membrane for Mg^{2+} and on the outside for Cs^+, Rb^+ or Ba^{2+}. We would, therefore, propose that the cardiac inwardly rectifying K^+ channel is composed of three identical conducting units, which usually function co-operatively or are regulated by a common gate to act as a single channel. Multi-barrel structures have also been suggested based on spontaneous sublevels of the open-channel current in other ion channels. The chloride-selective channel of *Torpedo electroplax* is composed of two subunits (Miller, 1982) and molluscan neurones contain a K^+ channel composed of a cluster of elementary channels (Kazachenko & Geletyuk, 1984). A large anion-selective channel of pulmonary alveolar epithelial cells consists of six parallel conducting pathways, which share a common regulatory gate that can occlude all six pathways simultaneously (Krouse, Schneider & Gage, 1986). The apical membrane of the distal tubule in the kidney of *Amphiuma* contains a K^+-selective channel made up of four parallel equally conductive subunits (Hunter & Giebisch, 1987).

Sublevels in the inward current were induced in about 20% of experiments by the external application of Cs^+ and Rb^+, and the remaining experiments showed simple transitions between the full open level and zero-conductance level. In two multi-channel recordings the application of Cs^+ induced sublevels in one of the channels, but other channels within the same patch did not show sublevels. We do not believe, however, that a fraction of channels are composed of three conductive units and others have only one ion pathway. First, no significant difference in the single-channel conductance was detected between the two groups. Second, the mean dwell time at the full open level coincided well in the two groups (Fig. 9), and the voltage dependence of the rate constants (δ) also agreed well (Figs 6 and 7). Third, in the previous study (Matsuda, 1988) sublevels were detected in all channels when micromolar Mg^{2+} was applied to the inner side of the membrane.

The difference in the two groups may be attributable to variations in the interaction between the elementary units. In one group of channels, the three

elementary units are blocked independently of the others. In the other group, as one of their partners is plugged by the blocking cation, the two non-blocked units close in a co-operative manner or by closure of a common gate, so as to be inaccessible to additional blockers (eqn (9)). We tested this simple hypothesis by comparing the mean dwell times at the zero-conductance level (right panel of Fig. 9) and the dissociation constants (Fig. 10) and have demonstrated that this model cannot fully explain the results.

Alternatively, the findings might be explained by assuming that the two non-blocked conductive units close simultaneously as the first unit is blocked, but remain accessible to blockers. The sequential scheme can be described as:

$$O_3 \underset{\lambda}{\overset{3\mu}{\rightleftharpoons}} B_2 \underset{2\lambda}{\overset{2\mu}{\rightleftharpoons}} B_1 \underset{3\lambda}{\overset{\mu}{\rightleftharpoons}} B_0, \tag{10}$$

where B_2, B_1, and B_0 are the non-conducting states in which one, two and all three of the units are plugged by blockers. In this scheme, the mean blocked time should be the sum of the dwell times in B_0, B_1 and B_2. To test this model, we measured the interval between two successive full openings in experiments with sublevels, neglecting the two-thirds and one-third levels, and compared it with the blocked time measured in experiments without sublevels (triangles in right panel of Fig. 9). The data points deviated from the theoretical line and thus this model also fails to explain the results without sublevels. At present we have no clear explanation of the interaction between the elementary units in the absence of sublevels. It may be assumed that the block of one of the elementary channels increases the unblocking rate in addition to closing the other conductive units.

External Cs^+ not only produced a flickering block of the channel current but also considerably decreased the long-lasting closures (Fig. 1). Measurement of the mean lifetimes of the open and closed states indicates that most of the transitions between the open level and the zero-conductance level are due to block and unblock during the open state of the channel. This fact facilitated our analysis of the blocking kinetics by Cs^+ and Rb^+. The sequential scheme given in eqn (1) implies that a blocked channel cannot close; closure can only occur from the open state. The rate constants calculated according to Kameyama *et al.* (1983) were $\alpha 1 = 88\ s^{-1}$, $\beta 1 = 7{\cdot}0\ s^{-1}$, $\alpha 2 = 1{\cdot}0\ s^{-1}$ and $\beta 2 = 13\ s^{-1}$ at E_r −60 mV. On the other hand, the blocking rate is $1120\ s^{-1}$ at the same membrane potential with 20 μM-Cs^+. Thus, in the presence of Cs^+, for a channel in the full open state, the probability of a transition to the blocked state is 99·3%, and that of a transition to C_1 is 0·7%.

The blocking rate by Rb^+ was smaller than that of Cs^+. The rate from the full open state to the blocked state (O_2 or B) was $35\ s^{-1}$ at E_r −60 mV with 20 μM-Rb^+. In this case, the probability of a transition from the full open state to O_2 or B is 83%, and that to C_1 is 17%. In fact, the closed-time histogram with external Rb^+ shows the long zero-current periods ascribed to the closed states C_1 and C_2 (e.g. O_0 in Fig. 5*B*).

Values of δ greater than one have been obtained in whole-cell current experiments in other preparations: 1·4–1·5 for Cs^+ in egg cells (Hagiwara *et al.* 1976) and 1·4 for Cs^+ and Rb^+ in skeletal muscle (Gay & Stanfield, 1977; Standen & Stanfield, 1980). They require a pore which can contain more than one ion at a time (Hille & Schwarz, 1978). On the other hand, δ values obtained in cardiac cells from single-channel

recordings are smaller than one: 0·3 for Mg^{2+} (Matsuda, 1988), 0·59 for Cs^+ and 0·14 for Rb^+ (the present study). Such a difference might result from differences in preparations or experimental methods.

The value of δ for Cs^+ was larger than that for Rb^+, both with and without sublevels. This may indicate that the blocking site for Cs^+ is located deeper in the channel pore (further from the outer mouth) than that for Rb^+, if the K^+ channel is considered as a series of energy barriers and wells (Hille & Schwarz, 1978; Ohmori, 1980). Unblocking rate constants for Cs^+ decreased with hyperpolarization from E_r -0 to -60 mV, but slightly increased with further hyperpolarization. This fact may be explained by assuming that Cs^+ can pass through all the energy barriers to the inner side of the membrane when the driving force is increased. The release of the block by Cs^+ at large hyperpolarizations, which was expressed as an increase of the unblocking rate constant, has been reported in the anomalous K^+ rectifier of preparations other than cardiac cells (Gay & Stanfield, 1977; Standen & Stanfield, 1980; Ohmori, 1980; Fukushima, 1982). Unblocking rate constants in Rb^+ block showed little voltage dependence. It is therefore reasonable to assume that the energy well for Rb^+ may be located near the outer mouth of the channel and that Rb^+ permeates poorly through inwardly rectifying K^+ channels in cardiac cells.

We thank Drs N. Standen, M. Shattock, T. Ehara and Y. Ikemoto for valuable comments on the manuscript. One of the authors (H. Matsuura) is grateful to Professor K. Tokunaga, Institute of Angiocardiology, for providing him with an opportunity to work at the Department of Physiology. The secretarial assistance of Fumiko Katsuda is gratefully acknowledged. This work was supported by grants from the Ministry of Education, Science and Culture of Japan and from 'The Research Program on Cell Calcium Signals in the Cardiovascular System'.

REFERENCES

FUKUSHIMA, Y. (1982). Blocking kinetics of the anomalous potassium rectifier of tunicate egg studied by single-channel recording. *Journal of Physiology* **331**, 311–331.

GAY, L. A. & STANFIELD, P. R. (1977). Cs causes a voltage-dependent block of inward K currents in resting skeletal muscle fibers. *Nature* **267**, 169–170.

HAGIWARA, S., MIYAZAKI, S., MOODY, W. & PATLAK, J. (1978). Blocking effects of barium and hydrogen ions on the potassium current during anomalous rectification in the starfish egg. *Journal of Physiology* **297**, 167–185.

HAGIWARA, S., MIYAZAKI, S. & ROSENTHAL, N. P. (1976). Potassium current and the effect of cesium on this current during anomalous rectification of the egg cell membrane on a starfish. *Journal of General Physiology* **67**, 621–638.

HAMIL, O. P., MARTY, A., NEHER, E., SAKMANN, B. & SIGWORTH, F. J. (1981). Improved patch-clamp techniques for high-resolution current recording from cells and cell-free membrane patches. *Pflügers Archiv* **391**, 85–100.

HILLE, B. & SCHWARZ, W. (1978). Potassium channels as multi-ion single-file pores. *Journal of General Physiology* **72**, 409–442.

HORIE, M. & IRISAWA, H. (1987). Rectification of muscarinic K^+ current by magnesium ion in guinea pig atrial cells. *American Journal of Physiology* **253**, H210–214.

HORIE, M., IRISAWA, H. & NOMA, A. (1987). Voltage-dependent magnesium block of adenosine-triphosphate-sensitive potassium channel in guinea-pig ventricular cells. *Journal of Physiology* **387**, 251–272.

HUNTER, M. & GIEBISCH, G. (1987). Multi-barrelled K channels in renal tubules. *Nature* **327**, 522–524.

IMOTO, Y., EHARA, T. & MATSUURA, H. (1987). Voltage- and time-dependent block of i_{K1} underlying Ba^{2+}-induced ventricular automaticity. *American Journal of Physiology* **252**, H325–333.

ISENBERG, G. & KLÖCKNER, U. (1982). Calcium tolerant ventricular myocytes prepared by preincubation in a 'KB medium'. *Pflügers Archiv* **395**, 6–18.

KAMEYAMA, M., KIYOSUE, T. & SOEJIMA, M. (1983). Single channel analysis of the inward rectifier K current in the rabbit ventricular cells. *Japanese Journal of Physiology* **33**, 1039–1056.

KAZACHENKO, V. N. & GELETYUK, V. I. (1984). The potential-dependent K^+ channel in molluscan neurons is organized in a cluster of elementary channels. *Biochimica et biophysica acta* **773**, 132–142.

KROUSE, M. E., SCHNEIDER, G. T. & GAGE, P. W. (1986). A large anion-selective channel has seven conductance levels. *Nature* **319**, 58–60.

KURACHI, Y. (1985). Voltage-dependent activation of the inward-rectifier potassium channel in the ventricular cell membrane of guinea-pig heart. *Journal of Physiology* **366**, 365–385.

MATSUDA, H. (1988). Open-state substructure of inwardly rectifying potassium channels revealed by magnesium block in guinea-pig heart cells. *Journal of Physiology* **397**, 237–258.

MATSUDA, H., SAIGUSA, A. & IRISAWA, H. (1987). Ohmic conductance through the inwardly rectifying K channel and blocking by internal Mg^{2+}. *Nature* **325**, 156–159.

MILLER, C. (1982). Open-state substructure of single chloride channels from *Torpedo electroplax*. *Philosophical Transactions of the Royal Society* B **299**, 401–411.

NEHER, E. (1983). The charge carried by single-channel currents of rat cultured muscle cells in the presence of local anaesthetics. *Journal of Physiology* **339**, 663–678.

OHMORI, H. (1980). Dual effects of K ions upon the inactivation of the anomalous rectifier of the tunicate egg cell membranes. *Journal of Membrane Biology* **53**, 143–156.

POWELL, T., TERRAR, D. & TWIST, V. W. (1980). Electrical properties of individual cells isolated from adult rat ventricular myocardium. *Journal of Physiology* **302**, 131–153.

SAKMANN, B. & TRUBE, G. (1984*a*). Conductance properties of single inwardly rectifying potassium channels in ventricular cells from guinea-pig heart. *Journal of Physiology* **347**, 641–657.

SAKMANN, B. & TRUBE, G. (1984*b*). Voltage-dependent inactivation of inward-rectifying single-channel currents in the guinea-pig heart cell membrane. *Journal of Physiology* **347**, 659–683.

SOEJIMA, M. & NOMA, A. (1984). Mode of regulation of the ACh-sensitive K-channel by the muscarinic receptor in rabbit atrial cells. *Pflügers Archiv* **400**, 424–431.

STANDEN, N. B. & STANFIELD, P. R. (1978). A potential and time-dependent blockade of inward rectification in frog skeletal muscle fibres by barium and strontium ions. *Journal of Physiology* **280**, 169–191.

STANDEN, N. B. & STANFIELD, P. R. (1980). Rubidium block and rubidium permeability of the inward rectifier of the frog skeletal muscle fibres. *Journal of Physiology* **304**, 415–435.

VANDENBERG, C. A. (1987). Inward rectification of a potassium channel in cardiac ventricular cells depends on internal magnesium ions. *Proceedings of the National Academy of Sciences of the USA* **84**, 2560–2564.